Multi-objective Dynamic Optimal Power Flow of Wind Integrated Power Systems Considering Demand Response

Rui Ma, *Member, IEEE*, Xuan Li, Yang Luo, Xia Wu, and Fei Jiang, *Member, IEEE*

***Abstract*—This paper studies the economic environmental energy-saving day-ahead scheduling problem of power systems considering wind generation (WG) and demand response (DR) by means of multi-objective dynamic optimal power flow (MDOPF). Within the model, fuel cost, carbon emission and active power losses are taken as objectives, and an integrated dispatch mode of conventional coal-fired generation, WG and DR is utilized. The corresponding solution process to the MDOPF is based on a hybrid of a non-dominated sorting genetic algorithm-II (NSGA-II) and fuzzy satisfaction-maximizing method, where NSGA-II obtains the Pareto frontier and the fuzzy satisfaction-maximizing method is the chosen strategy. Illustrative cases of different scenarios are performed based on an IEEE 6-units\30-nodes system, to verify the proposed model and the solution process, as well as the benefits obtained by the DR into power system.**

***Index Terms*—Demand response, low-carbon electricity, multi-objective dynamic optimal power flow, NSGA-II, wind generation.**

Nomenclature

A. WG and DR

t, T	Time period, time horizon.
$P_{\mathrm{WG}}^{\mathrm{fore}}$, P_{WC}, P_{WG}	Forecasting WG power, WG curtailment, actual WG output.
n_{DR}	Number of DRs.
$P_{\mathrm{DR}}^{\mathrm{cap}}$	Power capacity of DR.
ξ	Expense related to DR power capacity.
$P_{\mathrm{L}}^{\max}$	Maximum load of the power system.
$\varepsilon^{\max}, \varepsilon^{\min}$	Load percentages to decide DR status.
P_{DR}	Active power output of DR.
C_{DR}	Total expense on scheduling a DR.
$\zeta, \zeta^{+}, \zeta^{-}$	Electricity price for DR.
λ	Switch variable denoting the dispatch status of DR.

B. MDOPF

$\boldsymbol{u}$	Vector of control variables.
f	Objective function.
M	Number of objectives.
n_{G}	Number of coal-fired generations.
$P_{\mathrm{G}}, U_{\mathrm{G}}$	Active power injection and voltage of generation.
n_{SC}	Number of shunt capacitors.
B	Shunt susceptance value of shunt capacitor.
a, b, c	Cost coefficients of generation.
C_{G}	Expense on coal-fired generation.
$\alpha,\ \beta,\ \gamma$	Emission coefficients of generation.
n_{bus}	Number of system buses.
δ_{ij}	Phase difference between bus i and j.
G_{ij}, B_{ij}	Conductance and susceptance of the line between bus i and j.
$U, U^{\min}, U^{\max}$	Voltage, voltage limits.
$P_{\mathrm{G}}^{\min}$, $P_{\mathrm{G}}^{\max}$, $Q_{\mathrm{G}}^{\min}$, $Q_{\mathrm{G}}^{\max}$	Active and reactive power limits of generation.
$B^{\min}, B^{\max}$	Shunt susceptance limits.
$P_{\mathrm{L}}, Q_{\mathrm{L}}$	Active and reactive load.
σ	Spinning reserve percentage.
$P_{\mathrm{G}}^{\mathrm{down}}, P_{\mathrm{G}}^{\mathrm{up}}$	Ramp and descending rate limits of generation.
n_{L}	Number of system lines.
$S_{\mathrm{L}}, S_{\mathrm{L}}^{\max}$	Line power flow, power limits.

C. Algorithm

n_{PQ}	Number of system lines.
H	Penalty function.
Δ	Out-of-limit value.
cf	Synthesized objective function considering penalty function.
g	Current iteration times in NSGA-II.
h	Dynamic adjustment factor.
μ	Objective satisfaction.

I. Introduction

LOW-CARBON electricity has long been a core issue in power systems to cope with climate change, fossil energy shortage and environmental pollution [1]. So power scheduling should be planned considering both economic and environmental goals [2], [3]. Given the fact that power wastage is ubiquitous during transmission and sometimes can be pretty

Manuscript received March 11, 2017; revised May 6, 2017; accepted June 15, 2017. Date of publication December 30, 2019; date of current version November 4, 2019. This work was supported in part by the National Natural Science Foundation of China under Grant 51277015, 51677007 and 51977012.

R. Ma (corresponding author, email: marui818@126.com), X. Li, X. Wu, Y. Luo and F. Jiang are with the School of Electrical and Information Engineering, Changsha University of Science & Technology, Changsha 410114, Hunan.

DOI: 10.17775/CSEEJPES.2017.00280

considerable in large grid, minimizing power loss is also necessary to be taken into account [4].

Optimal power flow (OPF) [5], [6] is a method proposed to determine the generation schedule of the committed units so as to meet the load demand, with control variables adjusted to optimize specific objectives and simultaneously with respect to constraints on the network such as nodal power balance, bus voltage, etc. So a multi-objective OPF model is an appropriate way to mathematically describe optimal power scheduling. Many of the existing researches on multi-objective OPF with at least three or more objectives primarily relies on the approach of a static framework [7], which is used to optimize for a particular point in time. However, the day-ahead power scheduling plan should be made under the time horizon of a whole day, where the inter-temporal correlations such as generator ramp rate and load fluctuation need to be carefully considered. Therefore, researchers have proposed inter-temporal or dynamic optimal power flow (DOPF) which is an extended method to solve OPF across a time-horizon [8] by incorporating the inter-temporal constraints. Economic environmental energy-saving day-ahead power scheduling based on multi-objective dynamic optimal power flow (MDOPF) is of research value but is seldom reported.

Wind power generation (WG) as an application of the environmentally-friendly renewable wind energy, brings greater challenges to power system operations with its high penetration into the system [9]–[11], and its anti-peaking feature which may deteriorate the peak-valley differences of the daily net load curve [12]. This phenomenon threatens the stability of the power system and calls for more spinning reserve in case of emergencies. In addition, low-carbon efforts also gives rise to new resources on the user side such as distributed renewable energy with large-capacity energy storage devices which can sometimes generate energy for the network if under the management and regulation of the power system. Development of the smart grid and electricity market brings about a demand response (DR) strategy [13], [14]. An integrated dispatch scheme involving the two sides can be much more effective [15], [16], and DR is proved to be effective in cost savings, emission reduction, and load shifting [12]. With the participation of WG and DR, the variation and flexibility of the power system is increased, necessitating dynamic optimal scheduling research under such circumstances. S. Gill et al. [8] studied the DOPF problem of active distribution networks containing renewable energy, flexible demand and energy storage under an active network management context. Z. Bie et al. [17] and R. Ma et al. [18] established a day-ahead unit commitment model considering WG and DR.

MDOPF is a large-scale, nonlinear, non-convex optimization problem with both static and inter-temporal constraints, and the objectives in a multi-objective optimization problem are essentially restricted and conflicting. Researchers have studied and applied many mathematical optimization techniques especially heuristic optimization algorithms, such as differential evolution [19] and non-dominated sorting genetic algorithm-II (NSGA-II) [20]. In [18], the proposed dynamic multi-objective unit commitment problem is solved by NSGA-II to obtain Pareto optimal solutions, and the fuzzy satisfaction-maximizing method is adopted in decision-making.

In this paper, we studied an economic environmental energy-saving day-ahead scheduling model of a wind integrated power system considering DR as part of a MDOPF problem and proposed a solution process based on NSGA-II and the fuzzy satisfaction-maximizing method. First, a power system with WG and incentive-based DR is modeled. Next, a MDOPF framework considering WG and DR is built, with minimum generation cost, carbon emission and net loss as objectives. Then, the model's solving method is developed. Finally, a case study on MATLAB is conducted to prove the effectiveness and practicability of the model and proposed solving method.

II. Model for Power System with WG and DR

Day-ahead power scheduling for a wind integrated power system first requires load demand curve and WG output curve forecasting. Considering having excessive wind power curtailed, the WG output $P_{\mathrm{WG}}(t)$ is decided by:

$$P_{\mathrm{WG}}(t) = P_{\mathrm{WG}}^{\mathrm{fore}}(t) - P_{\mathrm{WC}}(t) \tag{1}$$

Equipped with an energy storage system and renewable energy system, the incentive-based DR is a typical type of interactive resource based on a program giving incentive payments to induce higher electricity usage in the valley load period and create generation to power systems in the peak [13]. An agreement between dispatchers department and consumers is signed declaring the power capacity $P_{\mathrm{DR}j}^{\mathrm{cap}}$ and the involved time periods. A related fee ξ_j $(j = 1, 2, \cdots, n_{\mathrm{DR}})$ is prepaid by the dispatch department. During the whole scheduling time horizon, DR behavior is needed when the power demand exceeds or drops below a certain percentage of $P_{\mathrm{L}}^{\max}$. Considering DR as a generation, its power output should be:

$$\begin{cases} P_{\mathrm{DR}j}(t) > 0, & P_{\mathrm{L}}(t) \geq \varepsilon^{\max} P_{\mathrm{L}}^{\max} \\ P_{\mathrm{DR}j}(t) < 0, & P_{\mathrm{L}}(t) \leq \varepsilon^{\min} P_{\mathrm{L}}^{\max} \end{cases} \tag{2}$$

Thus, the peak load can be reduced and the valley load is increased. This phenomenon is the so-called *load shifting*. Note that the DR with such a kind of quality is effective in accommodating wind power, especially faced with an *anti-peaking* WG output curve. The anti-peaking future means that the WG generates abundantly during the valley load period while poorly at the peak load time, which contradicts with *load shifting*. Based on the forecasting load curve, the dispatch department determines the day-ahead scheduling of the power system and informs consumers of the plan at length. Consumers can provide feedback to make some adjustments. Another part of the payment for consumers is calculated according to the power dispatched in this particular period. Thus, the total expense on scheduling a DR resource at tth period is:

$$C_{\mathrm{DR}j}(t) = \zeta_j(t) P_{\mathrm{DR}j}(t) + \lambda_j(t)\xi_j \tag{3}$$

where

$$\zeta_j(t) = \begin{cases} \zeta_j^{+}, & P_{\mathrm{DR}j}(t) > 0 \\ \zeta_j^{-}, & P_{\mathrm{DR}j}(t) < 0 \end{cases} \tag{4}$$

and

$$\lambda_j(t)=\begin{cases}1, & P_{\mathrm{DR}j}(t)\neq 0\\ 0, & \text{else}\end{cases} \tag{5}$$

III. MDOPF Model Considering Wind Generation and Demand Response

A MDOPF framework of a wind integrated power system with DR is designed as follows. The optimization horizon is for a whole day split up into $T(T=24)$ time periods. The control variable vector is $\boldsymbol{u}(t)=[P_{\mathrm{G}1}(t),\cdots,P_{\mathrm{G}n_G-1}(t), P_{\mathrm{DR}1}(t),\cdots,P_{\mathrm{DR}n_{\mathrm{DR}}}(t),P_{\mathrm{WC}}(t),U_{\mathrm{G}1}(t),\cdots,U_{\mathrm{G}n_G}(t), B_1(t),\cdots,B_{n_{\mathrm{SC}}}(t)]$, where $n_{\mathrm{G}}-1$ denotes that the active power of generation on the reference bus which is excluded.

A. Objectives

1) Minimize Generation Cost

$$f_1[\boldsymbol{u}(t)]=\min\sum_{t=1}^{T}\left\{\sum_{i=1}^{n_{\mathrm{G}}}C_{\mathrm{G}i}(t)+\sum_{j=1}^{n_{\mathrm{DR}}}C_{\mathrm{DR}j}(t)\right\} \tag{6}$$

where

$$C_{\mathrm{G}i}(t)=a_iP_{\mathrm{G}i}^2(t)+b_iP_{\mathrm{G}i}(t)+c_i \tag{7}$$

The WG regulation is deemed costless, so the optimization sums the generation cost of every coal-fired generation and dispatchable DR throughout the whole time horizon.

2) Minimize CO_2 Emission

$$f_2[\boldsymbol{u}(t)]=\min\sum_{t=1}^{T}\left\{\sum_{i=1}^{n_{\mathrm{G}}}[\alpha_iP_{\mathrm{G}i}^2(t)+\beta_iP_{\mathrm{G}i}(t)+\gamma_i]\right\} \tag{8}$$

We consider the wind power generation process and DR resource as pollution-free, so the objective sums only the carbon emission of the coal-fired generation units together, as shown in (8).

3) Minimize Active Power Loss

$$f_3[\boldsymbol{u}(t)]= \tag{9}$$
$$\min\sum_{t=1}^{T}\left\{\sum_{i=1}^{n_{\mathrm{bus}}}U_i(t)\sum_{j\in\Gamma}U_j(t)[G_{ij}\cos\delta_{ij}(t)+B_{ij}\sin\delta_{ij}(t)]\right\}$$

where $U_i(t)$ is the voltage of the bus i $(i=1,2,\cdots,n_{\mathrm{bus}})$ at tth period; Γ is the cluster of all buses connected with bus i.

B. Constraints

1) Static Constraints

For $\forall t=1,2,\cdots T$, it is required to ensure the following static constraints.

1) Power balance limits

$$\forall i=1,2,\cdots n_{\mathrm{bus}} \tag{10}$$
$$\begin{cases}P_{\mathrm{G}i}(t)-P_{\mathrm{L}i}(t)-\\ U_i(t)\sum\limits_{j\in\Gamma}U_j(t)[G_{ij}\cos\delta_{ij}(t)+B_{ij}\sin\delta_{ij}(t)]=0\\ Q_{\mathrm{G}i}(t)-Q_{\mathrm{L}i}(t)-\\ U_i(t)\sum\limits_{j\in\Gamma}U_j(t)[G_{ij}\sin\delta_{ij}(t)+B_{ij}\cos\delta_{ij}(t)]=0\end{cases}$$

2) Generation limits

$$P_{\mathrm{G}i}^{\min}\le P_{\mathrm{G}i}(t)\le P_{\mathrm{G}i}^{\max},\forall i=1,2,\cdots n_{\mathrm{G}} \tag{11}$$
$$Q_{\mathrm{G}i}^{\min}\le Q_{\mathrm{G}i}(t)\le Q_{\mathrm{G}i}^{\max},\forall i=1,2,\cdots n_{\mathrm{G}} \tag{12}$$

3) Bus voltage limits

$$U_i^{\min}\le U_i(t)\le U_i^{\max},\forall i=1,2,\cdots n_{\mathrm{bus}} \tag{13}$$

4) WG curtailment limits

$$P_{\mathrm{WC}}(t)\le P_{\mathrm{WG}}^{\mathrm{fore}}(t) \tag{14}$$

5) DR capacity limits

$$|P_{\mathrm{DR}j}(t)|\le P_{\mathrm{DR}j}^{\mathrm{cap}},\forall j=1,2,\cdots,n_{\mathrm{DR}} \tag{15}$$

6) Shunt susceptance limits

$$B_k^{\min}\le B_k(t)\le B_k^{\max},\forall k=1,2,\cdots,n_{\mathrm{SC}} \tag{16}$$

7) Branch power flow limits

$$S_{\mathrm{L}i}\le S_{\mathrm{L}i}^{\max},\forall i=1,2,\cdots,n_{\mathrm{L}} \tag{17}$$

8) Spinning reserve of power system

$$\sum_{i=1}^{n_{\mathrm{G}}}[P_{\mathrm{G}i}^{\max}-P_{\mathrm{G}i}(t)]+\sum_{j=1}^{n_{\mathrm{DR}}}[P_{\mathrm{DR}j}^{\mathrm{cap}}-P_{\mathrm{DR}j}(t)]\ge\sigma P_{\mathrm{L}}^{\max} \tag{18}$$

2) Dynamic Constraints

The active power ramp rate constraint of the coal-fired generations is:

$$-P_{\mathrm{G}i}^{\mathrm{down}}\le P_{\mathrm{G}i}(t+1)-P_{\mathrm{G}i}(t)\le P_{\mathrm{G}i}^{\mathrm{up}},\forall i,t \tag{19}$$

Considering the ramp rate limits, generation limits can be decided by:

$$\begin{cases}P_{\mathrm{G}i}^{\min}(t)=\max\{P_{\mathrm{G}i}^{\min},P_{\mathrm{G}i}(t-1)-P_{\mathrm{G}i}^{\mathrm{down}}\}\\ P_{\mathrm{G}i}^{\max}(t)=\min\{P_{\mathrm{G}i}^{\max},P_{\mathrm{G}i}(t-1)+P_{\mathrm{G}i}^{\mathrm{up}}\}\end{cases} \tag{20}$$

IV. Solution Process

The proposed MDOPF model, as an extension of a traditional OPF, has increased the number of control variable manifolds, and the inter-temporal constraints need to be dealt with. In addition, the three objectives are conflicting, which means the impossibility to have them all optimized in the same time frame. In this paper, the optimization is spilt into subproblems with their inter-temporal constraints and is solved by a corresponding solution process shown in Fig. 1. The mains steps are as follows:

1) Obtain day-ahead load and WG forecasting curve, and set $t=1$;

2) Status of coal-fired generations effected by the previous dispatch schedule is estimated, and the power output limits in the current time period are decided. By comparing the current power demand with $\varepsilon^{\max}P_{\mathrm{L}}^{\max}$ and $\varepsilon^{\min}P_{\mathrm{L}}^{\max}$, the dispatch state of the DR resources, whether as generation or load, is determined;

3) Apply NSGA-II to obtain Pareto optimal solutions, and decide the compromise optimal solution via the fuzzy satisfaction-maximizing method;

4) $t+1$, and judge if t has exceeded the schedule time horizon. If so, full day-ahead optimal scheduling is obtained; if not, return to step 2).

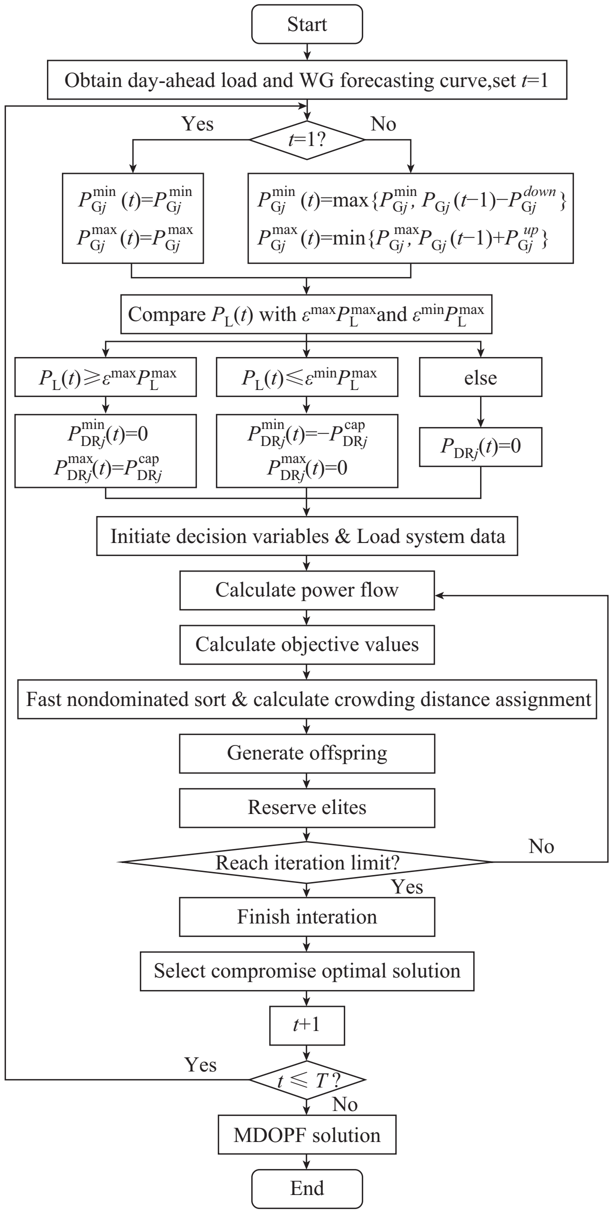

Fig. 1. Flowchart to solve MDOPF.

A. Penalty Function Method for State Variable Constraint in MDOPF

To ensure the constraints on the state variables such as bus voltage and reactive power generation limit, we applied the dynamic penalty function method based on the work in [21]. Note that the active power output of coal-fired generation on the reference bus is not the decision variable. Its power injection is acquired after the power flow calculation, so we consider it as one of the state variables.

It is necessary to determine if the PV bus reactive power, PQ bus voltage, reference bus power and generation ramp-rate are within their limits. If so, the corresponding penalty function of this section is set to 0. Otherwise, the penalty function is calculated as:

$$H_Q[\boldsymbol{u}(t)] = \sum_{i=1}^{n_G} \left[\frac{\Delta Q_{Gi}(t)}{Q_{Gi}^m}\right]^2 \tag{21}$$

$$H_U[\boldsymbol{u}(t)] = \sum_{i=1}^{n_{PQ}} \left[\frac{\Delta U_i(t)}{U_i^m}\right]^2 \tag{22}$$

$$\begin{aligned} &H_{Gp}[\boldsymbol{u}(t), \boldsymbol{u}(t-1)] \\ &= \left[\frac{\Delta P_{Gp}(t)}{P_{Gp}^m}\right]^2 + \left\{\frac{\Delta[P_{Gp}(t) - P_{Gp}(t-1)]}{\Delta P_{Gp}^m}\right\}^2 \end{aligned} \tag{23}$$

where the denominator represents the limit. If the upper bound is overstepped, the denominator is set as the upper bound. Conversely, it is set as the lower one. The numerator denotes the out-of-limit value.

The total penalty function is calculated by:

$$H[\boldsymbol{u}(t)] = H_Q[\boldsymbol{u}(t)] + H_U[\boldsymbol{u}(t)] + H_{Gp}[\boldsymbol{u}(t), \boldsymbol{u}(t-1)] \tag{24}$$

During NSGA-II optimizing, the non-dominated sort and crowding distant assignment proceed based on the calculation of the synthesized objective $cf_m[\boldsymbol{u}(t)]$

$$cf_m[\boldsymbol{u}(t)] = f_m[\boldsymbol{u}(t)] + h(g) \cdot H[\boldsymbol{u}(t)] \tag{25}$$

where $f_m[\boldsymbol{u}(t)]$ denotes the value of the objective $m(m = 1, 2, \cdots M)$; g is the current iteration times in NSGA-II; $h(g) = g\sqrt{g}$ is the dynamic adjustment factor which increases with the iteration accumulation. Thus, the synthesized objective of the scheme with out-of-limit variables is enlarged dramatically, and the scheme is to be eliminated during the optimization.

B. Three-dimensional Pareto Optimal Frontier and Synthetically Optimal Solution

Based on genetic thought, NSGA-II is an advanced algorithm which can reach Pareto optimality via non-dominated sorting techniques and the crowding distance operator. Pareto optimal sets of a triple-objective optimization problem form a Pareto frontier in three-dimensional space, with each non-dominated solution referring to a schedule in this period. The three-dimensional Pareto frontier can indicate the macroscopic relationship among the three objectives. The Pareto frontier contains rich information, providing decision makers with whatever they prefer to choose.

Among all the feasible solutions in the Pareto front, a synthetically optimal one is chosen through the fuzzy satisfaction-maximizing method. For a single non-dominated solution numbered by n, the satisfaction μ_m^n of each objective value is calculated by a falling semi-trapezoidal fuzzy set function [18]:

$$\mu_m^n = \begin{cases} 1, & f_m \le f_{m\min} \\ \dfrac{f_{m\max} - f_m}{f_{m\max} - f_{m\min}}, & f_{m\min} \le f_m \le f_{m\max} \\ 0, & f_m \ge f_{m\max} \end{cases} \tag{26}$$

where $f_{m\min}$, $f_{m\max}$ are the maximum and the minimum value of objective m in the Pareto solution set, respectively.

Then the total fuzzy satisfaction μ^n of the nth non-dominated solution in the Pareto frontier is calculated by (27) and the one with the maximum value is selected.

$$\mu^n = \left(\sum_{m=1}^{M} \mu_m\right) / \left(\sum_{n=1}^{N}\sum_{m=1}^{M} \mu_m\right) \tag{27}$$

V. Case Study

We carry out a case study based on an IEEE 6-units\30-nodes system on MATLAB, with a 24-h optimization horizon split up into 1-hour time-steps and with two scenarios:

1) Power systems with traditional coal-fired generations and a wind farm at bus 8;

2) As for scenario 1, three DR resources are added at bus 2, 8 and 22, respectively.

The system outline is as shown in Fig. 2. Both the wind farm and DRs are located at the buses with relatively larger power demand. The day-ahead forecasting system load [22] and WG power output profile are shown in Fig. 3. Power demand at each bus typically drops before dawn and climbs in the morning. The WG output is a representative anti-peaking profile from a wind farm in China, to simulate the worst circumstances. Parameters for the coal-fired generations are listed in Table I.

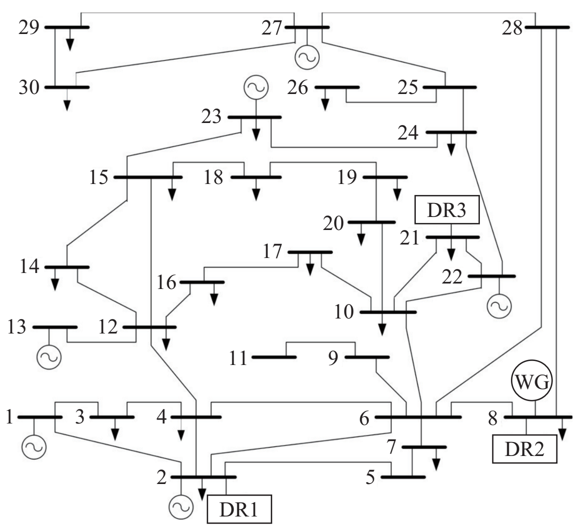

Fig. 2. Schematic diagram based on 6-units\30-nodes system.

In scenario 1, coal-fired generations and WG regulation are available with the means to be dispatched. Without WG regulation, i.e. WG output and the daily load form the power demand from coal-fired generations, the anti-peaking WG output would deteriorate the peak-valley differences by digging the demand curve's valley while barely ameliorating the peak load condition. If the demand drops to a level in which all coal-fired generations need to break their lower limits on power output, grid reliability is jeopardized. And the sudden rise of power demand in the morning may require unrealistic ramp rates for coal-fired generations. Therefore, only by curtailing wind power can the grid maintain supply-demand balance and reliability, as in scenario 1. Since wind curtailment causes energy waste and frequent operations, one purpose to introduce DR is to help handle the problems. Related parameters for DR resources in scenario 2 are listed in Table II.

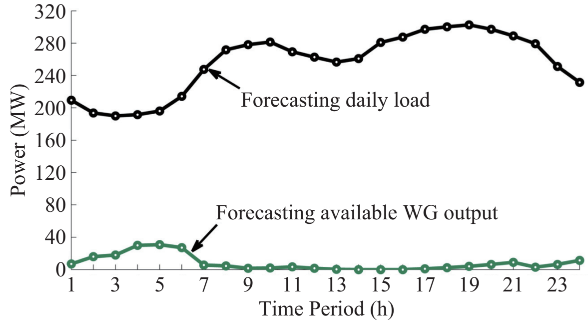

Fig. 3. Forecasting system load and WG output profiles.

TABLE II
Parameters of DR Resources

DR j	Bus i	$P_{\mathrm{DR}j}^{\mathrm{cap}}$ MW	ζ_j^+ \$/(MW·h)	ζ_j^- \$/(MW · h)	ξ_j \$
1	2	15	5	−3	10
2	8	20	5.5	−3	15
3	21	10	6	−4	10

Within NSGA-II, we set the population size as 100, Pareto fraction as 0.35 and generations as 500. Examples of Pareto frontiers in scenario 1 and 2 during simulation are shown in Fig. 4 and Fig. 5. Each dot refers to a feasible dispatch scheme which satisfies constraints on the generation and network. Single dots form a line indicating that reducing CO_2 emission

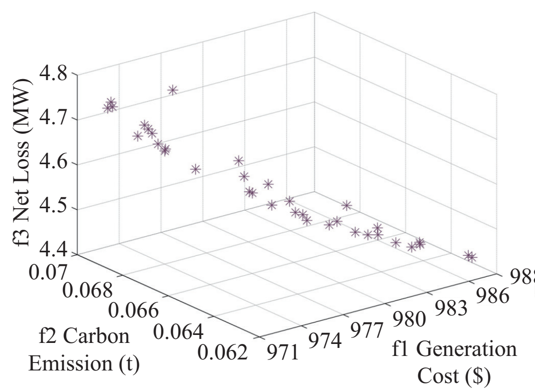

Fig. 4. Three-dimensional Pareto frontier, Scenario 1, 15th period.

TABLE I
Parameters of Coal-fired Generations

Gen i	Bus i	$P_{\mathrm{G}i}^{\max}$ MW	$P_{\mathrm{G}i}^{\min}$ MW	$Q_{\mathrm{G}i}^{max}$ MVar	$Q_{\mathrm{G}i}^{\min}$ MVar	$P_{\mathrm{G}i}^{\mathrm{up}}$ MW	$P_{\mathrm{G}i}^{\mathrm{down}}$ MW	a_i $\$/(\mathrm{MW}^2\cdot\mathrm{h})$	b_i $\$/(\mathrm{MW}\cdot\mathrm{h})$	c_i \$/h	α_i $\mathrm{t}/(\mathrm{MW}^2\cdot\mathrm{h})$	β_i $\mathrm{t}/(\mathrm{MW}\cdot\mathrm{h})$	γ_i t/h
1	1	80	40	150	−20	20	20	0.02	2	0	6.490×10^{-6}	-5.554×10^{-6}	4.091×10^{-6}
2	2	80	40	60	−20	20	20	0.0175	1.75	0	3.380×10^{-6}	-3.550×10^{-6}	5.326×10^{-6}
3	22	50	25	62.5	−15	13	13	0.0083	3.25	0	5.638×10^{-6}	-6.047×10^{-6}	2.543×10^{-6}
4	27	55	30	48.7	−15	14	14	0.0250	3	0	4.568×10^{-6}	-5.094×10^{-6}	4.258×10^{-6}
5	23	40	20	40	−10	10	10	0.0250	3	0	4.568×10^{-6}	-5.094×10^{-6}	4.257×10^{-6}
6	13	50	30	44.7	−15	15	15	0.0625	1	0	3.245×10^{-6}	-2.777×10^{-6}	2.045×10^{-6}

will increase generation cost, along with reducing power loss. In scenario 2, when pursuing economic goals, the generation cost can be lowered to 1022.40$, with 0.6038 t CO_2 emission and 4.5681 MWh power loss. Likewise, the environmental aim will be best achieved with high monetary expense. Comparing the solution of minimum generation cost with the one of minimum CO_2 emission, we find that CO_2 emission can be cut by 0.01374 t with a 29.37$ increase in generation cost, meanwhile net loss can be reduced by 0.1655 MWh, which is beneficial to the electric line maintenance.

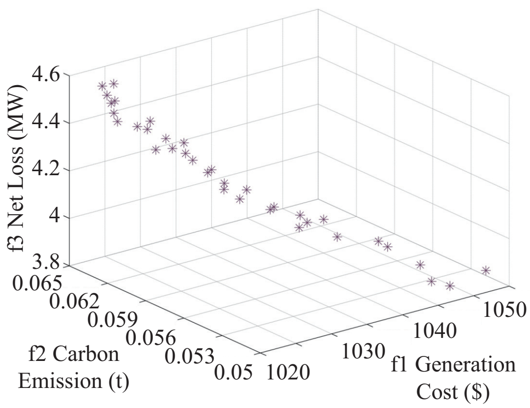

Fig. 5. Three-dimensional Pareto frontier, Scenario 2, 15th period.

Listed in Table III are day-ahead solutions of the two given scenarios. Comparison of the solutions implies that CO_2 emission and net loss in scenario 2 are 0.1127 t and 4.1255 MWh lower than that in scenario 1, while generation cost increases by 448.28$. The calculations point out that, with DRs participating, the optimizing result can achieve 8.79% reduction in CO_2 emission and 4.55% reduction in net loss, by increasing 2.19% of the power generation cost.

TABLE III
OBJECTIVE VALUES OF OPTIMAL SOLUTIONS

Objective value	Scenario 1	Scenario 2
Generation cost ($)	20467.91	20916.19
CO_2 emission (t)	1.2823	1.1696
Net loss (MW·h)	90.6068	86.4813

Detailed day-ahead scheduling solutions for scenario 1 and scenario 2 are shown in Fig. 6 and Fig. 7. Power output curves for generations in scenario 1 are more fluctuant than in scenario 2, especially generation 2 with an obvious decline during 11 to 13 periods and three times that of the large ramp or decent close to the limit. Through data analysis, it is found that the total ramp power of all generations throughout the whole day is 591.8358 MW in scenario 1 while it is 577.8710 MW in scenario 2. So, the DR's behavior can mitigate the power fluctuation of coal-fired generations. In scenario 2, negative values of DRs in the valley period denote that they need to absorb power from the system. Furthermore, during the valley period, considering the fact that wind power output brings about a sudden fall in power demand of the WG connected bus, which would definitely cause voltage and stability problems on this very bus if no measure is taken, a DR resource is introduced here to better accommodate the wind power. The simulation result turns out to show that, each DR, whether in the WG connected bus or not, have similar schedules. Thus, by means of MDOPF, the burden on one particular bus can be shared by other participants throughout the whole system. WG power injection into the grid would not cause that much impact on the optimal scheduling of the local DR resources, as we may have considered.

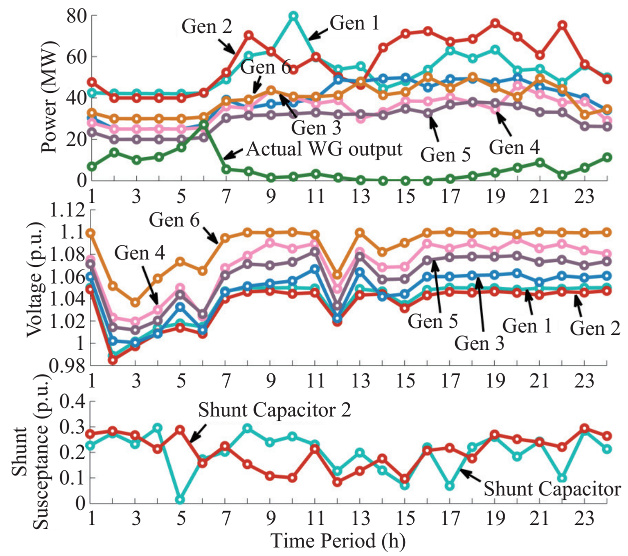

Fig. 6. Optimal day-ahead scheduling for scenario 1.

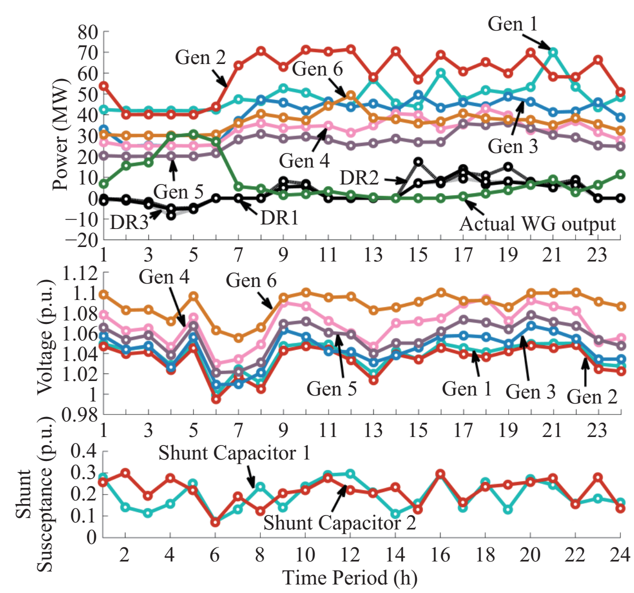

Fig. 7. Optimal day-ahead scheduling for scenario 2.

WG schedules of the two solutions are compared and are shown in Fig. 8 and Table IV. Obviously, curtailment of wind power is remarkably reduced when DR participates. Data analysis proves that, wind power curtailment in scenario 2 is 21.52% less than that in scenario 1. And utilization of wind power has been increased from 76.78% to 98.3%. With a better utilization of renewable energy achieved, the DR's capability to accommodate wind power is manifested. It is noteworthy that the WG output curve in this case study represents a worst-case scenario among all actual possibilities. Still, wind power can be well accommodated, showing the effectiveness of the proposed model and solution process.

TABLE IV
WG CURTAILMENT AND PEAK-VALLEY DIFFERENCE OF LOAD

		Scenario 1	Scenario 2
WG curtailment	(MW·h)	44.5281	3.2678
	(%)	23.22	1.70
Peak-valley difference of net load	(MW)	112.61	79.22

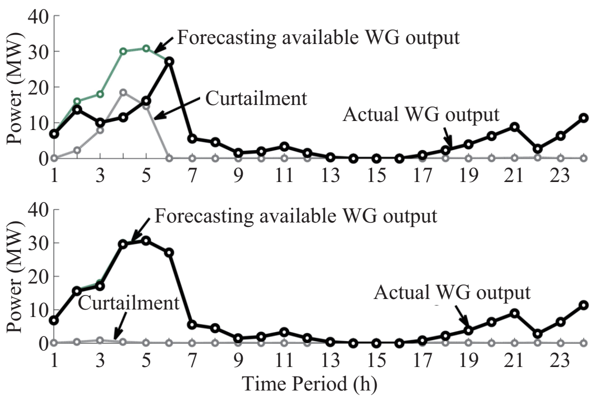

Fig. 8. WG schedule curves comparison.

Figure 9 compares system net load under two scenarios. In scenario 2, net load is obtained by adding DR to the fixed load demand. DR's schedule can alleviate peak-valley differences of the net load curve, by reducing it by almost 30% of scenario 1.

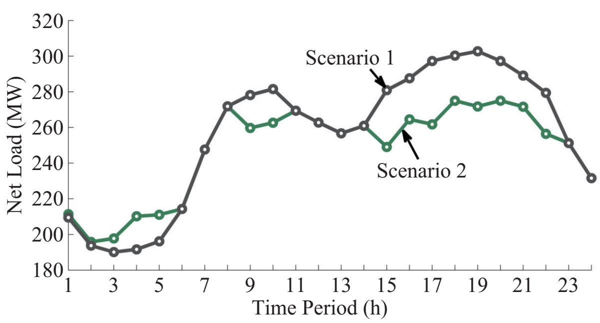

Fig. 9. Net load comparison.

VI. CONCLUSION

This paper presents a MDOPF model for day-ahead scheduling of wind integrated power systems with DR and proposes a solution method based on a hybrid of NSGA-II and fuzzy satisfaction-maximizing theory. Through the case study and analysis, it is shown that:

1) The integrated dispatch mode of a conventional coal-fired power generation, WG and DR is effective to accommodate wind power, alleviate peak-valley differences of the load curve as well as carbon emission reduction.

2) DR's participating can help coordinate the conflicting objectives by promoting low-carbon and low-loss benefits.

3) By investigating an extreme situation of the WG output curve, simulation results of the case study highlights DR's capability in accommodating wind power and the shifting load.

The model and the solution method this paper presents are proved to be of effective and practical value. WG uncertainty is to be considered in future research.

REFERENCES

[1] Q. X. Chen, C. Q. Kang, Q. Xia, and D. B. Guan, "Preliminary exploration on low-carbon technology roadmap of China's power sector," *Energy*, vol. 36, no. 3, pp. 1500–1512, Mar. 2011.

[2] R. Zhang, J. Z. Zhou, L. Mo, S. Ouyang, and X. Liao, "Economic environmental dispatch using an enhanced multi-objective cultural algorithm," *Electric Power Systems Research*, vol. 99, pp. 18–29, Jun. 2013.

[3] S. R. Konda, L. K. Panwar, B. K. Panigrahi, and R. Kumar, "A multiple emission constrained approach for self-scheduling of GENCO under renewable energy penetration," *CSEE Journal of Power and Energy Systems*, vol. 3, no. 1, pp. 63–73, Mar. 2017.

[4] R. Balamurugan and S. Subramanian, "An improved dynamic programming approach to economic power dispatch with generator constraints and transmission losses," *Journal of Electrical Engineering and Technology*, vol. 3, no. 3, pp. 320–330, Sep. 2008.

[5] H. W. Dommel and W. F. Tinney, "Optimal power flow solutions," *IEEE Transactions on Power Apparatus and Systems*, vol. PAS-87, no. 10, pp. 1866–1876, Oct. 1968.

[6] Y. D. Yang, Z. B. Wu, Y. Y. Zhang, and H. Wei, "Large-scale OPF based on voltage grading and network partition," *CSEE Journal of Power and Energy Systems*, vol. 2, no. 2, pp. 56–61, Jun. 2016.

[7] M. Ghasemi, S. Ghavidel, M. M. Ghanbarian, M. Gharibzadeh, and A. A. Vahed, "Multi-objective optimal power flow considering the cost, emission, voltage deviation and power losses using multi-objective modified imperialist competitive algorithm," *Energy*, vol. 78, pp. 276–289, Dec. 2014.

[8] S. Gill, I. Kockar, and G. W. Ault, "Dynamic optimal power flow for active distribution networks," *IEEE Transactions on Power Systems*, vol. 29, no. 1, pp. 121–131, Jan. 2014.

[9] Z. Chen, "Wind power in modern power systems," *Journal of Modern Power Systems and Clean Energy*, vol. 1, no. 1, pp. 2–13, Jun. 2013.

[10] J. K. Lyu, J. H. Heo, M. K. Kim, and J. K. Park, "Impacts of wind power integration on generation dispatch in power systems," *Journal of Electrical Engineering and Technology*, vol. 8, no. 3, pp. 453–463, May 2013.

[11] A. J. Conejo, Y. H. Cheng, N. Zhang, and C. Q. Kang, "Long-term coordination of transmission and storage to integrate wind power," *CSEE Journal of Power and Energy Systems*, vol. 3, no. 1, pp. 36–43, Mar. 2017.

[12] B. B. Wang, X. C. Liu, and Y. Li, "Day-ahead generation scheduling and operation simulation considering demand response in large-capacity wind power integrated systems," *Proceedings of the CSEE*, vol. 33, no. 22, pp. 35–44, Aug. 2013.

[13] M. H. Albadi and E. F. El-Saadany, "A summary of demand response in electricity markets," *Electric Power Systems Research*, vol. 78, no. 11, pp. 1989–1996, Nov. 2008.

[14] H. G. Yan, B. Li, S. S. Chen, M. Zhong, D. Z. Li, L. M. Jiang, and G. X. He, "Future evolution of automated demand response system in smart grid for low-carbon economy," *Journal of Modern Power Systems and Clean Energy*, vol. 3, no. 1, pp. 72–81, Mar. 2015.

[15] H. W. Zhong, Q. Xia, Y. Xia, C. Q. Kang, L. Xie, W. He, and H. L. Zhang, "Integrated dispatch of generation and load: a pathway towards smart grids," *Electric Power Systems Research*, vol. 120, pp. 206–213, Mar. 2015.

[16] H. J. Xing, H. Z. Cheng, and L. B. Zhang, "Demand response based and wind farm integrated economic dispatch," *CSEE Journal of Power and Energy Systems*, vol. 1, no. 4, pp. 37–41, Dec. 2015.

[17] Z. H. Bie, H. P. Xie, G. W. Hu, and G. F. Li, "Optimal scheduling of power systems considering demand response," *Journal of Modern Power Systems and Clean Energy*, vol. 4, no. 2, pp. 180–187, Apr. 2016.

[18] R. Ma, K. Li, X. Li, and Z. Y. Qin, "An economic and low-carbon day-ahead Pareto-optimal scheduling for wind farm integrated power systems with demand response," *Journal of Modern Power Systems and Clean Energy*, vol. 3, no. 3, pp. 393–401, Sep. 2015.

[19] B. Mahdad and K. Srairi, "A study on multi-objective optimal power flow under contingency using differential evolution," *Journal of Electrical Engineering and Technology*, vol. 8, no. 1, pp. 53–63, Jan. 2013.

[20] M. Rajkumar, K. Mahadevan, S. Kannan, and S. Baskar, "NSGA-II technique for multi-objective generation dispatch of thermal generators with nonsmooth fuel cost functions," *Journal of Electrical Engineering and Technology*, vol. 9, no. 2, pp. 423–432, Mar. 2014.

[21] W. Yang, B. A. Teng, and L. Sun, "Optimal power flow model and its algorithm in environment of electricity market," *Power System Technology*, vol. 36, no. 2, pp. 126–130, Feb. 2012.

[22] Z. N. Wei, Y. P. Xiang, G. Q. Sun, and X. Q. Huang, "Carbon emission-considered multi-objective dynamic optimal power flow of power system containing carbon-capture plant," *Power System Technology*, vol. 36, no. 12, pp. 11–17, Dec. 2012.

Rui Ma (M'11) received a B.Sc. degree in Electrical Engineering from Changsha University of Electric Power, Changsha, Hunan, China, in 1994, a M.Sc. degree in Control Theory and Control Engineering from Hunan University, Changsha, Hunan, China, in 1999, and a Ph.D. degree in Electrical Engineering from North China Electric Power University, Beijing, China, in 2006. He was a visiting scholar at Texas A&M University, TX, USA from September 2009 to July 2011.

Presently, he is a Professor in the School of Electrical and Information Engineering, Changsha University of Science and Technology. His research interests are power system security analysis, renewable energy accessing, electricity market, and low-carbon electricity.

Xuan Li received a B.Sc. degree in Electrical Engineering from Changsha University of Science and Technology, Changsha, Hunan, China, in 2014. She is now pursuing a M.Sc. degree in Electrical Engineering at Changsha University of Science and Technology, Changsha, Hunan, China. Her research interests include optimal power flow and low-carbon electricity.

Yang Luo received a B.Sc. degree in Civil Engineering from Central South University of Forestry and Technology, Changsha, Hunan, China, in 2011, and a M.Sc. degree in Electrical Engineering at Changsha University of Science and Technology, Changsha, Hunan, China, in 2015. His research interests include power system demand response and low-carbon electricity.

Xia Wu received a B.Sc. degree in Electrical Engineering from Changsha University of Science and Technology, Changsha, Hunan, China, in 2014. She is now pursuing a M.Sc. degree in Electrical Engineering at Changsha University of Science and Technology, Changsha, Hunan, China. Her research interest is power system modeling and high penetrated wind power generation.

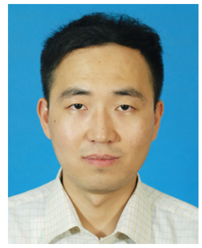

Fei Jiang (S'15–M'16) received B.S and M.S. degrees in Electrical and Information Engineering from Changsha University of Science and Technology, Changsha, China, in 2007 and 2012 respectively, and a Ph.D. degree in Electrical Engineering from Hunan University, Changsha, China, in 2016.

He is currently a lecturer in the School of Electrical and Information Engineering, Changsha University of Science and Technology. His research interests include power quality control, power electronics, and power system security analysis.